ingegneria sismica
International Journal of Earthquake Engineering
Anno XLIII - Num. 2 - 2026

An improved graph convolutional neural network model is used for fault detection of the main circulation pump of the valve cooling system of the converter station

Yang Li[1], *Zhiqiang Liu*[1], *Chunhai Guo*[1], *Jing Gan*[2], *Yingying Lv*[3,*] *and Qiang Wang*[4]

[1] Ehv Transmission Companies Dali Office of China Southern Power Grid, Dali 671000, Yunnan, China
[2] School of Information, Yunnan University, Kunming 650091, China
[3] School of Information Engineering and Automation, Kunming University of Science and Technology, Kunming 650500, Chian
[4] Henan Jingrui Cooling Technology Co., LTD, Xuchang 461000, Henan, Chian

SUMMARY: *In the valve cooling system of converter station, the main circulation pump monitoring method based on fixed threshold is easy to ignore the coupling changes between pressure, flow, motor current, vibration and temperature signals. This paper proposes an improved graph Convolutional neural Network (IGCN) for pump fault detection under cooling load changes. 38640 synchronous operation records were collected from the two converter stations, covering normal operation, flow attenuation, pressure fluctuation, bearing vibration, seal leakage, and motor current abnormalities. Each sensor channel is represented as a graph node, and adaptive edge weights are calculated based on operational correlation, device connectivity, and fault response delay. The temporal residual aggregation was embedded into the graph convolution propagation process to retain the short-term fluctuation pattern. The dataset is divided into training, validation and test sets at 8:1:1. Experimental results show that IGCN achieves 96.1% accuracy, 94.8% recall rate and 95.6% F1 value, and the average inference delay is 38 ms, which supports stable online fault detection applications of valval-cooled pump.*

KEYWORDS: *Improved graph convolutional neural network; Converter station valve cooling system; Main circulation pump; Fault detection*

1 Introduction

The valve cooling system of converter station undertakes the tasks of heat exchange, medium circulation and temperature stability of converter valve components. The main circulation pump is the core equipment to maintain the continuous output of cooling water flow and pressure. Bearing wear, mechanical seal leakage, impeller blockage, current fluctuation and line pressure mutation will change the hydraulic state of the valve cold circuit and affect the heat dissipation margin. The existing station monitoring mostly relies on fixed threshold, single point alarm and manual inspection, which can find the out-of-limit state, but it is difficult to express the linkage changes between pressure, flow, vibration, temperature and current. The main circulation pump fault is usually not a single signal surge, but a shift between multiple measurement points. For such conditions, multivariate relational model is

*yingyinglv_kust@163.com
https://doi.org/10.65102/is20261028
Published: 30 April, 2026

suitable for identification.

Focusing on the fault detection of rotating equipment, Cheng et al. studied the unsupervised fault detection method of the planetary gearbox of the nuclear circulating pump, and used the generalization feature to describe the abnormal state of the circulating pump equipment when the fault label was missing [1]. Zhang et al. proposed pruning optimization weighted graph convolutional network to introduce hydrophone signals into axial flow pump fault diagnosis, and enhance equipment signal correlation expression through weighted graph structure [2]. Kovalenko et al. proposed graph neural network with trainable adjacency matrix for fault diagnosis of multivariate sensor data, so that the relationship between equipment measurement points no longer depends on manual setting [3]. Brahmbhatt et al. proposed a fault detection method combining graph autoencoder and attention graph convolution to enhance the ability to identify abnormal propagation paths in industrial process data [4]. Seo et al. studied anomaly detection and diagnosis of graph neural network in hydrogen extraction system, indicating that graph structure learning is suitable for dealing with multi-device and multi-measurement point coupling system [5].

The fault diagnosis research of pump equipment also provides the basis for the state identification of main circulating pump. Zaman et al. proposed a centrifugal pump fault diagnosis method combining dual-scale atlas, convolutional autoencoder and artificial neural network, and used time-frequency representation for pump body anomaly identification [6]. Ullah et al. proposed an intelligent diagnosis framework for centrifugal pumps based on wavelet coherence analysis and deep learning to enhance the correlation description of vibration signals under different fault states [7]. Manikandan and Duraivelu studied the vibration diagnosis method of impula fracture and mechanical seal failure of industrial single centrifugal pump, and used deep convolutional neural network to complete fault classification [8]. Ahmad et al. proposed a fault-specific Mann-Whitney test method for centrifugal pump fault detection and identification to improve the ability of feature selection and state differentiation [9]. Zaman et al. proposed a centrifugal pump fault diagnosis method combining SobelEdge scalogram and convolutional neural network, so that the pump body signal could be converted into image input suitable for deep network processing [10]. The above studies show that deep learning has been able to deal with the fault characteristics of pump equipment, but the valve cold main circulation pump of converter station has the characteristics of strong load fluctuation, tight coupling of measurement points, and short alarm response time, so a model oriented to multi-sensor topological relationship is still needed.

Aiming at the structural correlation of operation signals of valve-cooled main circulation pump, this paper proposes an improved graph convolutional neural network fault detection model. The model maps measurement points such as pressure, flow, temperature, current and vibration into graph nodes, generates edge weights according to operational correlation, spatial arrangement and fault-sensitive distance, and adds dynamic adjacency update and time series residual aggregation to the graph convolution propagation, so that local fluctuations, inter-measurement point conduction and working condition changes can enter the classification calculation. The research contributions include: constructing a multi-point state diagram for valve-cooled main circulation pump, and forming a computational link from the acquisition signal to the fault feature map; A dynamic adjacent weight update method was designed to adjust the relationship between measuring points with the change of load. A graph convolution structure fused with time series residual was proposed to enhance the expression ability of early faults. The performance of the model in terms of precision, recall, F1 value and inference delay is verified by fault detection experiments.

2 Related work

Fault detection of the main circulation pump in the valve cooling system of converter station belongs to the cross task of intelligent operation and maintenance of power equipment and industrial multi-sensor diagnosis. The main circulation pump operation is affected by cooling load, pipeline resistance, valve group heat dissipation and mechanical state, pressure, flow, motor current, vibration, temperature and other signals will be linked in the same loop. Traditional threshold monitoring can identify the obvious out-of-limit data, but it is difficult to describe the conduction relationship between the measurement points. In recent years, deep learning, sequential networks and graph neural networks have gradually entered the fault detection scene of rotating machinery, which provides a technical basis for online identification of valve-cold pumps. The existing achievements mainly focus on four directions: pump vibration diagnosis, bearing degradation prediction, industrial multi-source signal fusion and anomaly detection.

Ahmad et al. studied the supervised contrastive learning framework in centrifugal pump fault diagnosis, compressing similar operating states into similar embedding regions, and extending the feature distance between different fault categories, so that pump vibration signals form a stable discriminant boundary in depth space [11]. Maliuk et al. proposed a hybrid feature selection framework based on Wrapper-WPT to screen out redundant frequency band information after wavelet packet decomposition for sensitive feature reservation in bearing fault diagnosis [12]. Afridi et al. studied the LSTM condition monitoring and fault prediction method based on raw vibration data, and used the cyclic structure to record the continuous changes during bearing degradation [13]. Zabin et al. proposed a transfer learning architecture for industrial fault diagnosis combining Hilbert transform and DCNN-LSTM, so that time-frequency analysis results, convolutional features and sequence dependence were jointly involved in classification [14]. These methods provide a reference for the signal processing of the valve-cooled main circulation pump. However, most of the studies focus on a single vibration link, which is difficult to directly express the spatial correlation of multiple measurement points in the valve-cooled loop.

Siddique et al. proposed a bearing fault classification method combining Mel scalogram and FOX optimization artificial neural network, which converted acoustic signals into two-dimensional expressions suitable for network learning and improved the separability of frequency structure [15]. Zaman et al. studied the differences in the application of VGG16, ResNet50 and wavelet coherence analysis in centrifugal pump fault diagnosis, indicating that the responses of different depth structures to pump fault signals are not consistent [16]. Umar et al. proposed a milling machine fault diagnosis method combining acoustic emission and hybrid deep learning, and used feature optimization to reduce the interference of irrelevant signals on classification results [17]. Praveen Kumar et al. evaluated the deep learning performance of vibration, sound and acoustic emission signals in rotating machinery fault diagnosis, and proved that the joint use of multi-source signals is more suitable for describing the state of complex equipment than a single signal [18]. These studies promote the development of multi-signal fusion diagnosis, and also show that the valve cold main circulation pump detection cannot rely on a single sensor threshold.

Al-Andoli et al. proposed a parallel ensemble learning model for fault detection and diagnosis of industrial machinery, and improved the classification stability through the joint output of multiple learners [19]. Bonci et al. proposed DeepESN neural network to realize industrial predictive maintenance by anomaly detection of production energy consumption data, indicating that non-vibration operation data also has the value of state identification [20].

Kermenov et al. proposed a dynamic system anomaly detection and concept drift adaptation method, and completed the verification in the industrial cooperative robot, which provides a reference for online diagnosis under the change of operation distribution [21].

To compare the connections between the existing studies and the proposed method, Table 1 summarizes the methods, data types, technical results, and directions that can be used for reference. The table shows that the existing research has formed a relatively mature deep feature extraction route, but the expression of measurement point topology, working condition switching and multi-parameter coupling conduction in the valve cooling system of the converter station is still not sufficient.

Table 1: Comparison of related work

Reference	Method	Data Type	Main Result	Relevance to This Study
[11]	Supervised contrastive learning	Centrifugal pump vibration data	Strengthened class boundaries	Supports pump state embedding
[12]	Wrapper-WPT feature selection	Bearing vibration signals	Removed redundant frequency-band information	Supports sensitive feature selection
[13]	LSTM-based state prediction	Raw vibration sequences	Described degradation dependencies	Supports temporal residual design
[14]	DCNN-LSTM transfer learning	Industrial fault signals	Enhanced cross-device adaptability	Supports generalization under complex operating conditions
[15]	Mel-scalogram and optimized ANN	Bearing acoustic signals	Identified frequency patterns	Supports signal spectrogram representation
[16]	Wavelet coherence and deep models	Centrifugal pump signals	Compared multiple network structures	Supports pump fault experiments
[17]	Acoustic emission and feature optimization	Milling equipment signals	Improved fault classification	Supports multi-source signal processing
[18]	Performance evaluation of deep models	Vibration, sound, and acoustic emission	Compared diagnostic performance	Supports multi-signal metric design
[19]	Parallel ensemble learning	Industrial machinery data	Enhanced detection stability	Supports baseline model setting
[20]	DeepESN anomaly detection	Production energy data	Served predictive maintenance	Supports online anomaly identification
[21]	Concept drift adaptation	Dynamic system data	Adapted to distribution changes	Supports operating-condition update mechanism

In the valve cooling system of converter station, the pump group load, cooling water and valve group heat will change the data distribution, and the model needs to adjust the measurement point relationship while maintaining the real-time inference speed. The improved graph convolutional neural network can represent the inlet pressure, outlet pressure, mother tube flow, motor current, pump body vibration and medium temperature as graph nodes, and describe their mutual influence through edge weights. Compared with the ordinary convolutional network and recurrent network, the graph convolution structure is more suitable for expressing the propagation characteristics of valve-cold pump faults in hydraulic circuits and electromechanical links. Based on the above research basis, this paper combines the dynamic neighboring weight, time series residual aggregation and fault classification layer to build an online detection model for the main circulation pump, so that the operation state of the valve-cooling system can form a learnable, updatable and traceable fault representation in the computer model.

3 Fault detection method of main circulation pump based on improved graph convolutional neural network

3.1 Fault signal extraction and abnormal state calibration of valve-cooled main circulation pump

The main circulation pump of the valve cooling system of the converter station undertakes the task of continuous delivery of cooling medium. The state of the pump body will be reflected in the inlet pressure, outlet pressure, female pipe flow, motor current, bearing vibration and medium temperature and other measurement points. In the fault signal extraction stage, the multi-channel operation at the same sampling time is put into the uniform time coordinate, and the state fragments that can be read by the computer model are formed. At the acquisition end, the monitoring quantity, protection quantity and inspection quantity are aligned according to the second-level timestamp, and the adjacent stable segment is used to interpolate the short-term packet loss, and the outlier value is retained to avoid the miscleaning of early fault fluctuations, and the data boundary is clearer.

In order to keep signals of different dimensions participating in state recognition in the same calculation scale, it is necessary to modify the steady-state baseline of the amplitude of each measurement point and retain the relative offset before and after the fault. The normalized sequence of measured points reflects the current amplitude and its relative offset. The calculation process is as follows:

$$s_i(t) = \frac{x_i(t) - \mu_i^0}{\sigma_i^0 + \varepsilon} \tag{1}$$

where $x_i(t)$ represents the original sampling value of the i measurement point at time t, μ_i^0 and σ_i^0 represent the mean and standard deviation of the measurement point in the healthy running sample, ε is the stability term to prevent the denominator from being too small, and $s_i(t)$ is the standard state value after the baseline correction is done. Instead of simply scaling the data, the function of this equation is to convert different physical quantities such as pressure, flow, current, and vibration into comparable offsets with respect to the health state, providing a unified input for subsequent anomaly calibration.

Fig. 1 illustrates the calculated path of the fault signal of the valve-cooled main circulation pump from the original measurement point to the anomaly calibration module. The left side

shows the data of pressure, flow, current, vibration and temperature in the monitoring system of the station. In the middle part, time alignment, steady-state baseline correction, fluctuation amplitude calculation and abnormal candidate segment interception are completed in turn.

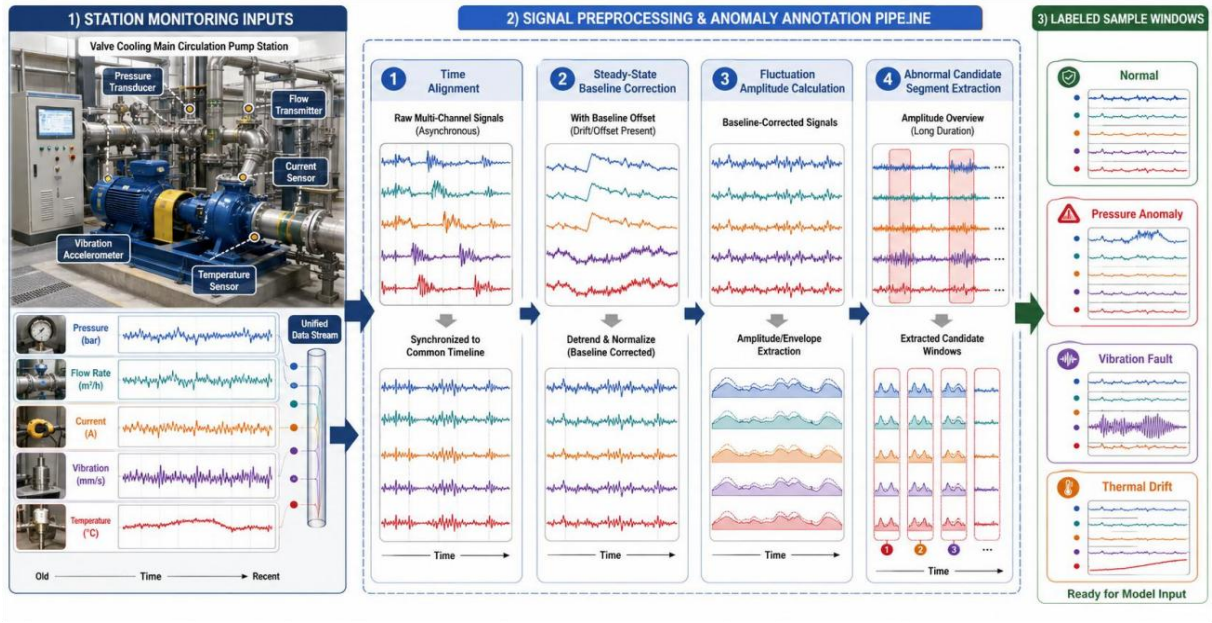

Figure 1: Fault signal extraction process of valve-cooled main circulation pump

In the extraction of abnormal candidate segments, the early fault of the main circulation pump often manifests as amplitude shift, increase of change rate and asynchrony of response between measurement points. To avoid concealment of minor faults by a single amplitude index, in this paper, the offset intensity, change gradient and overbound mark are combined into a fault sensitivity coefficient. The calculation process is as follows:

$$r_i(t) = \alpha|s_i(t)| + \beta|s_i(t) - s_i(t - \Delta t)| + \gamma b_i(t) \tag{2}$$

where $r_i(t)$ represents the fault sensitivity coefficient of the i measurement point, α, β, γ are the contribution weights of the three types of features, Δt represents the adjacent sampling interval, $b_i(t)$ is a binary quantity whether the measurement point triggers the regular marker at the station. This formula puts the stable offset, rapid fluctuation and engineering threshold information into the same expression, so that the subsequent model can read the data-driven features and the field operation rules at the same time.

Abnormal state calibration requires mapping continuous signal segments into normal, flow attenuation, pressure fluctuation, bearing vibration, seal leakage, and motor current abnormal categories. In order to reduce the boundary instability caused by manual calibration, this paper uses the joint score of multiple measurement points for label generation, and only when several measurement points show consistent offset in the same time window, the sample is classified into the fault category. The calculation process is as follows:

$$p_c(\tau) = \frac{\exp(\eta_c^T R(\tau) + \rho_c)}{\sum_{u=1}^{C} \exp(\eta_u^T R(\tau) + \rho_u)} \tag{3}$$

Here, $p_c(\tau)$ represents the probability that the time window τ belongs to the c class state, $R(\tau)$ is the statistical vector composed of fault sensitivity coefficients of all measurement points in the window, η_c and ρ_c represent the category mapping parameters,

and C is the number of state categories. This formula is used to form trainable soft labels, so that the probability difference between similar fault types is retained, and the interference of hard labels on model training is reduced.

Fig. 2 shows the anomaly state calibration and the sample archiving structure. In the figure, the upper part shows the main circulation pump operation segments segmented by time, and the lower part shows the state probability calculation, manual review of boundaries, and label archiving modules. The normal segment, the slight abnormal segment and the clear fault segment enter different buffers respectively. The sample number records the pump number, working condition, measuring point state and label source at the same time, so that the subsequent graph convolutional network can trace the generation basis of each fault sample

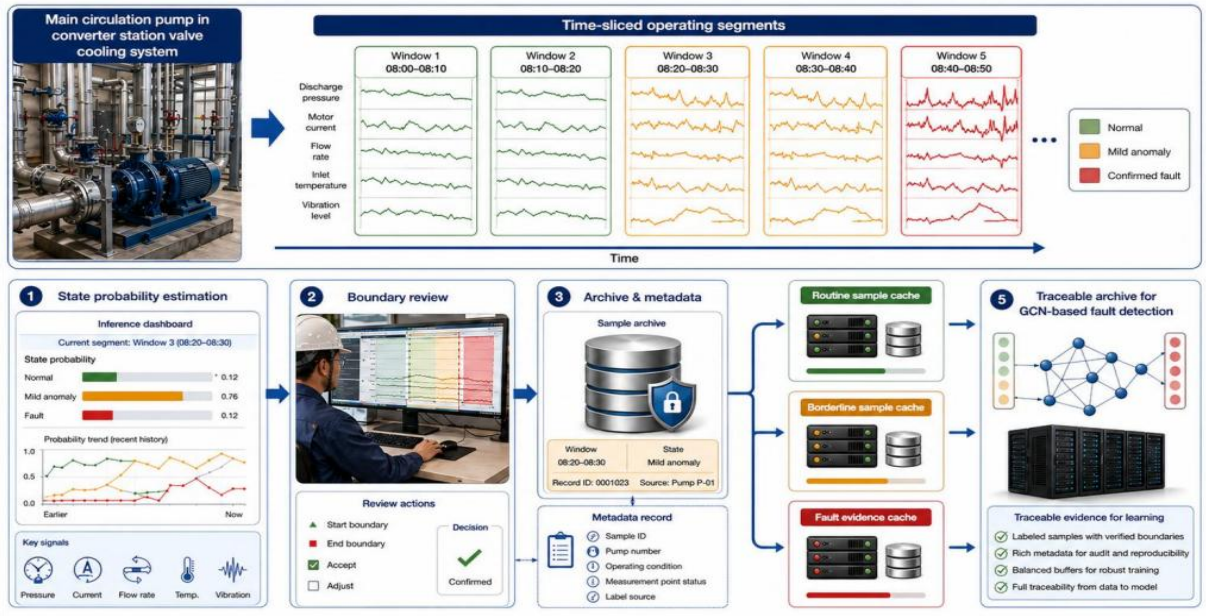

Figure 2: Anomaly state calibration and sample archive structure

After completing the probability mapping, the system needs to write the window samples to the training labels. In order to ensure that the calibration results are consistent with the on-site maintenance records, this paper sets confidence boundaries and review rules, and does not enter the training set for low confidence Windows. The process of determining the final state label is shown in the following equation:

$$y(\tau) = \begin{cases} \arg\max_c p_c(\tau), & \max_c p_c(\tau) \geq \theta \\ \emptyset, & \max_c p_c(\tau) < \theta \end{cases} \tag{4}$$

Here, $y(\tau)$ represents the final state label of window τ, θ represents the calibration confidence threshold, and $\emptyset$ represents the temporary review sample. This formula makes the training data only absorb the fault segments with clear boundaries, and avoids the condition switching, start-stop disturbance and short-time drift of sensors from mixing into the fault category. Through this process, the original operation signal of the valvecooled main circulation pump is converted into a standard sample with status label, which lays a data foundation for the subsequent topological mapping of measurement points and the generation of fault feature maps.

After the above processing, the original operation signal of the valvecooled main circulation pump is converted into a sample window with a uniform time scale, a uniform

amplitude reference, and a clear state label. This process preserves abnormal offsets in pressure, flow, current, vibration and temperature signals and also avoids miscalibration caused by single threshold judgment. After fault signal extraction and abnormal state calibration, each sample contains records of measuring point status, fault sensitivity coefficient, class probability and confidence, which provide stable input for subsequent topological mapping of measuring points.

3.2 Topology mapping and fault feature map generation of main circulation pump measurement points

The goal of the main circulation pump measurement point topology mapping is to convert the monitoring quantity originally scattered on the pipeline, motor and pump body in the valve cooling system into the graph structure input. Inlet pressure, outlet pressure, mother pipe flow, cooling water temperature, motor current, bearing vibration, and pump temperature rise are defined as graph nodes, and the connections between nodes are determined not only based on physical distance, but also based on operational correlation and failure response order. In this way, the generated feature map can retain the hydraulic conduction, electromechanical coupling and thermal state changes of the valve cold circuit, so that the improved graph convolutional network can obtain structural information closer to the field working conditions during calculation. On this basis, the feature map generation process also needs to keep the sample granularity consistent to avoid the deviation of node meaning caused by the difference of sampling frequency at different measurement points. In this paper, the statistical characteristics, engineering connections and response delays in the same window are encapsulated in a unified way, so that the subsequent convolution propagation no longer stays at the channel splicing level, but can be calculated along the valve cold loop structure, and the graph samples are stable and reliable.

In order to ensure that each measurement point node contains stable and learnable state information, this paper extracts the amplitude mean, fluctuation variance, change slope and frequency band energy from each time window to form the initial features of the node. This node feature vector is used to describe the running state of the measurement point within the local window. The calculation process is as follows:

$$z_i(\tau) = [\bar{s}_i(\tau),\ v_i(\tau),\ g_i(\tau),\ e_i(\tau)] \tag{5}$$

Here, $z_i(\tau)$ represents the node characteristics of the i measurement point within window τ, $\bar{s}_i(\tau)$ is the standardized signal mean, $v_i(\tau)$ is the fluctuation variance, $g_i(\tau)$ is the trend slope between the endpoints of the window, and $e_i(\tau)$ is the energy of the target frequency band. This formula compresses the continuous sampling into a structured node vector, which not only reduces the original sequence noise, but also retains the amplitude, fluctuation and trend information required for fault identification.

Fig. 3 shows the topological mapping relationship of the main circulation pump measurement points. In the figure, the pump inlet, pump outlet, mother tube, bearing housing, motor end and cooling medium temperature points are mapped as different nodes, and edges are formed between nodes according to the medium flow direction, equipment connection and signal correlation. The pressure and flow nodes reflect the hydraulic link, the current and vibration nodes reflect the electromechanical link, and the temperature node records the change of the heat dissipation state.

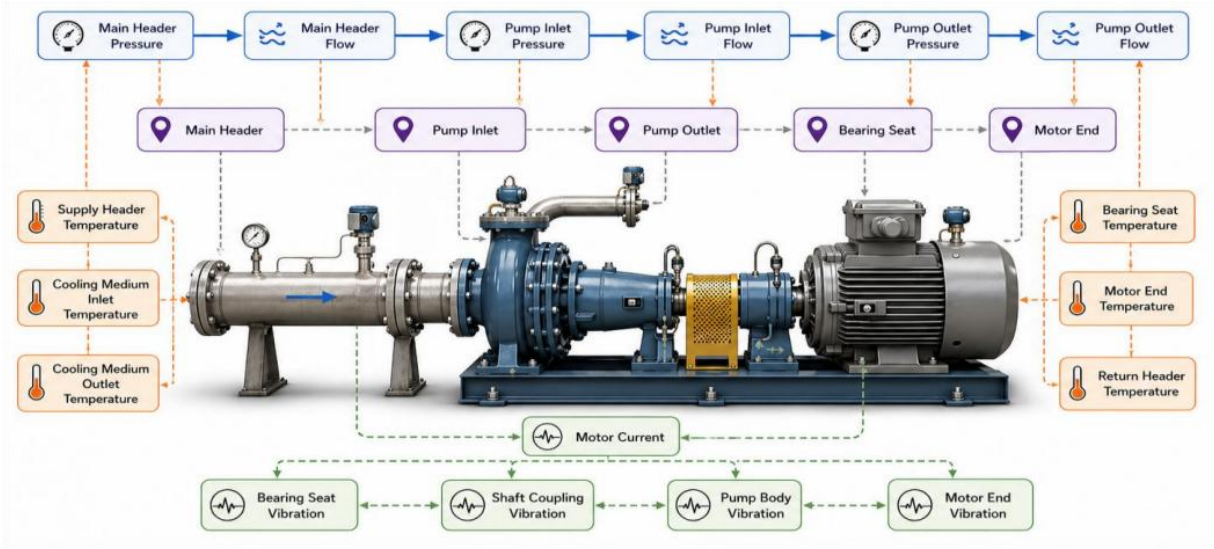

Figure 3: Topological mapping relation of measuring points of main circulation pump

Edge weight calculation determines whether the fault feature map can accurately express the influence strength between measurement points. In this paper, statistical correlation, physical connection distance and fault response delay are jointly incorporated into edge weight generation, so that neighboring measurement points and strong coupling measurement points can obtain higher connection weights in the graph. The edge weights are calculated as follows:

$$a_{ij}(\tau) = \sigma\left(\lambda_1 \kappa_{ij}(\tau) + \lambda_2 d_{ij}^{-1} + \lambda_3 \ell_{ij}^{-1}\right) \tag{6}$$

Here, $a_{ij}(\tau)$ represents the edge weight between measurement point i and measurement point j in window τ, $\sigma(\cdot)$ is the compression function, $\kappa_{ij}(\tau)$ represents the window correlation coefficient, d_{ij} represents the distance of measurement point on the device connection, ℓ_{ij} represents the anomaly response delay, and λ_1 to λ_3 are the weight coefficients. This formula enables the graph structure to absorb both data dependence and engineering connection relations, avoiding relying entirely on artificial topology or relying entirely on statistical dependence.

In actual operation, the correlation of measurement points will change due to the change of cooling load, so the adjacency relationship needs to be updated with the window. In this paper, a smooth update method is used to generate the dynamic adjacency matrix, so that the current working condition relationship and the historical stable relationship are jointly involved in the calculation. The update process is as follows:

$$A(\tau) = \omega A(\tau - 1) + (1 - \omega)\tilde{A}(\tau) \tag{7}$$

Here, $A(\tau)$ represents the adjacency matrix used in the current window, $A(\tau - 1)$ represents the adjacency matrix of the previous window, $\tilde{A}(\tau)$ represents the candidate matrix recalculation obtained from the correlation of the current measurement points, and ω is the smoothing coefficient. The formula can suppress the edge weight mutation caused by short-term disturbance, and retain the influence of working condition change on the measurement point relationship, which is suitable for the online detection scene of valve-cooled main circulation pump.

Fig. 4 shows the fault feature map generation process. The left input is the window sample

that completes the abnormal calibration, the middle part completes node feature extraction, edge weight calculation, smooth update of adjacency matrix and graph sample encapsulation in turn, and the right output can enter the fault feature map of the improved graph convolutional network. Each graph sample records the node feature matrix, dynamic adjacency matrix, state label and window index at the same time, so that the model training and detection results can be traced back to the specific running segment

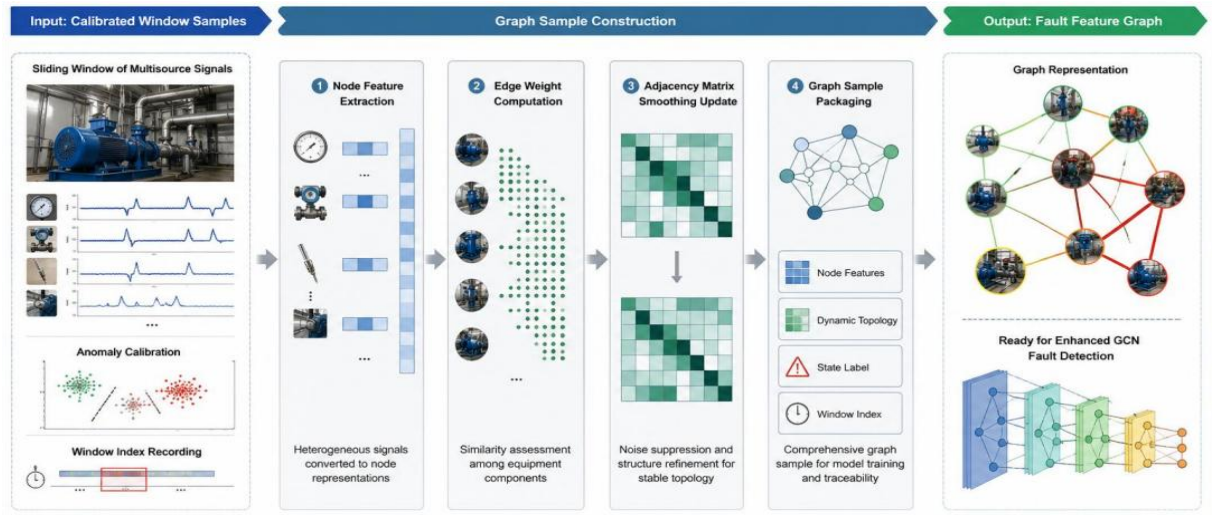

Figure 4: Fault feature map generation process

In order to synthesize node features and topological relationships as network input, we encapsulate node matrix, adjacency matrix and state label as a unified graph sample. Graph samples are generated as follows:

$$\mathcal{G}_\tau = (\mathrm{V}_\tau, \mathrm{A}(\tau), \mathrm{Z}(\tau), \mathrm{y}(\tau)) \tag{8}$$

Here,$\mathcal{G}_\tau$ represents the fault feature map corresponding to window τ, V_τ represents the collection of measuring point nodes, $\mathrm{Z}(\tau)$ represents the matrix composed of all node features, and $\mathrm{y}(\tau)$ represents the state label of this window. The equation completes the conversion from multi-channel operating signals to graph structure samples, so that the fault state of the main circulation pump can be jointly expressed by nodes, edges and labels, which provides complete input for the improvement of graph convolutional neural network.

Through the topological mapping of measurement points and the generation of fault feature graph, the operation data of the main circulation pump no longer enters the model in the form of ordinary multi-channel matrix, but is organized as a graph sample containing node characteristics, edge weight relationship, dynamic adjacency matrix and fault labels. The structure can express the correlation changes among hydraulic parameters, electromechanical parameters and thermal states in the valve cold circuit, so that the improved graph convolutional neural network can carry out feature propagation along the measurement point relationship in the subsequent calculation, and provide a structured basis for the identification of abnormal working conditions of the main circulation pump.

3.3 Improving the graph Convolutional neural Network fault detection model

3.3.1 Graph convolution feature propagation for valve cold pump measurement point association

The convolutional feature propagation of valve-cold pump measurement point correlation graph takes the fault feature graph as input, considers each measurement point as a node with operating attributes, and converts hydraulic connection, electromechanical coupling, and temperature response into edge-weight relationship. The inlet pressure, outlet pressure, mother tube flow rate, motor current, pump vibration and medium temperature are not simply concatenated in the model, but spread hierarchically along the adjacency matrix. In this way, the abnormal bearing vibration can affect the current node, and the flow attenuation can synchronously affect the pressure node, so that the graph convolution results are closer to the actual fault conduction process of the valve-cooled main circulation pump. The propagation layer adds a time series residual term on the basis of ordinary graph convolution, which not only retains the local fluctuations of the previous window, but also avoids the excessive smoothing of node differences after deep propagation. In order to keep the direction and strength of the pump group measurement point relationship consistent in the convolution propagation, the graph feature update is calculated by the adjacency weighted residual and constrained, as shown in the following equation:

$$P^{(l+1)}(\tau) = \phi\left(\widehat{A}(\tau)P^{(l)}(\tau)\Theta_l + Q^{(l)}(\tau)\Omega_l\right) \tag{9}$$

Here, $P^{(l+1)}(\tau)$ represents the feature matrix of measurement points after propagation at the $l+1$ th layer, $\widehat{A}(\tau)$ represents the dynamic adjacency matrix with self-connection, $P^{(l)}(\tau)$ represents the node input of the current layer, Θ_l represents the graph convolution mapping parameter, $Q^{(l)}(\tau)$ represents the time series residual extracted from adjacent Windows, Ω_l represents the residual mapping parameter. Let $\phi(\cdot)$ denote the nonlinear activation function. This equation puts the spatial propagation and time retention in the same layer, so that the model can not only transmit anomalies along the valve cold pump measurement point topology, but also retain short-term shocks and sustained offsets.

Fig. 5 shows the convolutional feature propagation structure of the correlation graph of the valve cold pump measurement points. The left side shows the fault feature graph input, the middle part shows the dynamic adjacency constraint, graph convolution propagation, timing residual compensation and layer normalization processing, and the right side outputs the graph-level representation for classification. Pressure, flow, current, vibration and temperature nodes maintain independent meaning in the graph, and edge weights participate in propagation according to operational correlation and fault response strength.

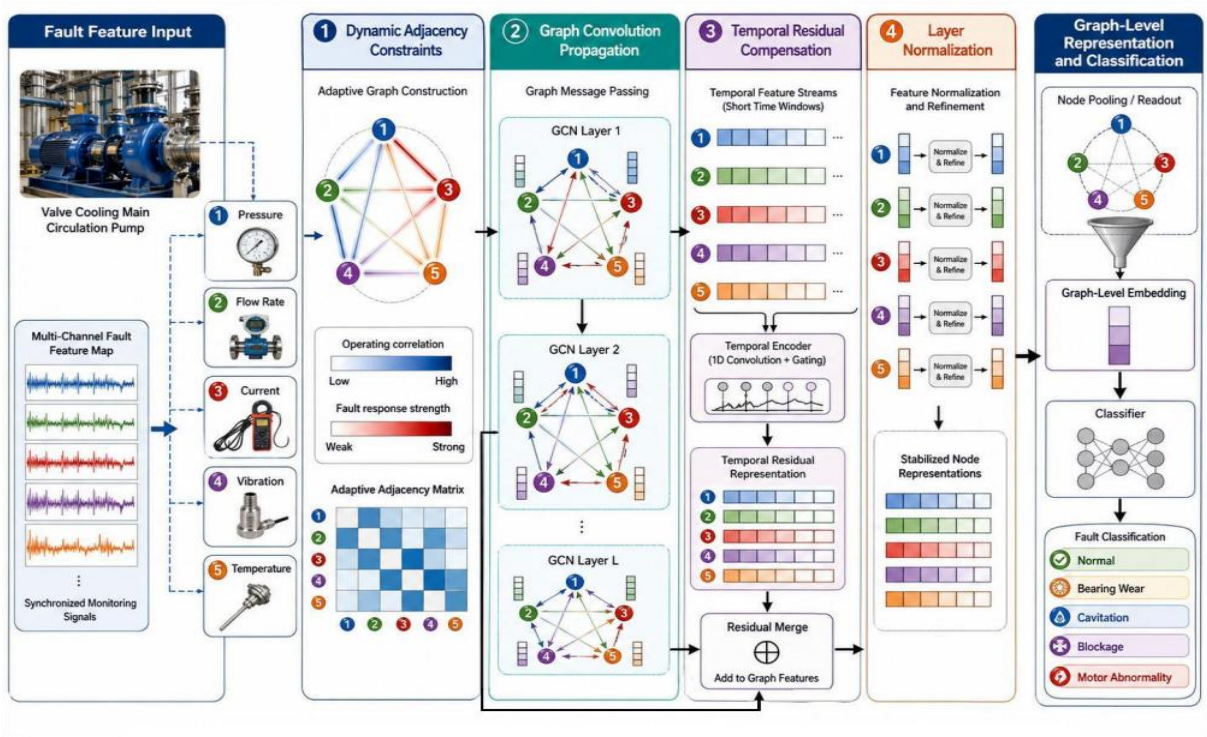

Figure 5: Convolutional feature propagation structure of correlation graph of valve cold pump measurement points

In multi-point fault propagation, different nodes do not have the same contribution to the target node. The seal leakage is more dependent on flow and pressure changes, the bearing anomaly is more dependent on vibration and current changes, and the motor overload is manifested as a combination of current, temperature rise and flow response. In order to describe the unbalanced influence between pressure, flow, current, vibration and temperature, the propagation weight between nodes introduces associated attention allocation and constrains the path set, as shown in the following equation:

$$\pi_{ij}^{(l)}(\tau) = \frac{a_{ij}(\tau)\exp\left((u_i^{(l)} \cdot u_j^{(l)})/\sqrt{d}\right)}{\sum_{k\in V_\tau} a_{ik}(\tau)\exp\left((u_i^{(l)} \cdot u_k^{(l)})/\sqrt{d}\right)} \tag{10}$$

Here, $\pi_{ij}^{(l)}(\tau)$ represents the attention weight propagated from node j to node i in layer l, $u_i^{(l)}$ and $u_j^{(l)}$ represent the hidden features before node propagation, and d represents the hidden dimension. This formula redistributes propagation contributions based on the existing edge weights, avoids excessive interference of weak correlation measurement points in fault classification, and also makes strong correlation measurement points obtain higher weight in the abnormal diffusion stage.

After the multi-layer graph convolution is completed, the model needs to compress the node-level features into a window-level representation. The fault state of the valve-cooled main circulation pump is determined by multiple measurement points, so the readout layer simultaneously retains the maximum response, mean state, and fault sensitive weighted results. In order to convert the multi-layer propagation results into a classifiable window representation, the model performs global readout and weighted aggregation of node features and stabilizes the output, as shown in the following equation:

$$g_\tau = \mathrm{concat}\left(\max_i P_i^{(L)}, \mathrm{mean}_i P_i^{(L)}, \sum_i \chi_i P_i^{(L)} \right) \tag{11}$$

Here, g_τ represents the graph-level representation corresponding to window τ, $\max_i P_i^{(L)}$ represents the maximum response in the node features of the last layer, $\mathrm{mean}_i P_i^{(L)}$ represents the node mean state, $\sum_i \chi_i P_i^{(L)}$ represents the global response weighted by the fault sensitivity coefficient χ_i, and $\mathrm{concat}(\cdot)$ represents vector concatenation. The formula can simultaneously preserve the strong abnormal nodes, the overall operating status and the contributions of key measurement points, so that the subsequent classification layer can read a more complete state expression of the valve cold pump.

To ensure the computational stability during online detection, the propagation layer records the node contribution value after each window update. If a measurement point maintains high response in a continuous window, the model will retain its contribution track in the graph-level representation, so that the subsequent alarm results can be traced back to the specific measurement point and the corresponding time segment. This processing can reduce the perturbation of the classification boundary by the transient noise and make the slight degradation signal of the pump group be expressed continuously before entering the classification layer. After the above propagation process, the model no longer relies on single point threshold or single channel sequence, but uses the structure of the measuring point diagram to describe the conduction relationship of the main circulation pump fault. The feature propagation results preserve the association differences in the hydraulic, electromechanical, and thermal response links, which provide stable input for the fault classification algorithm under abnormal operating conditions.

3.3.2 Fault classification algorithm for abnormal working condition of main circulation pump

The fault classification algorithm for abnormal operating conditions of the main circulation pump receives the graph-level representation of the output of the previous subsection and maps it to states such as normal, flow attenuation, pressure fluctuation, bearing vibration, seal leakage, and abnormal motor current. In the classification stage, the result of graph convolution is not directly equivalent to the alarm result, but the class probability is calculated first, and then the risk score and condition constraints are combined to generate the final discrimination. In this way, false alarms caused by start-stop switching, sudden change of cooling load and short-time sensor jitter can be avoided. The temperature adjustment mechanism was used in the output layer of the model to maintain the distinguishable probability boundary between similar fault classes. In order to map the propagated fault graph representation to a specific state category, the classification layer uses the probability output with temperature adjustment and stabilizes the correction boundary, as shown in the following equation:

$$\hat{p}_c(\tau) = \frac{\exp((r_c^\top g_\tau + b_c)/T)}{\sum_{u=0}^{C-1} \exp((r_u^\top g_\tau + b_u)/T)} \tag{12}$$

Here,$\hat{p}_c(\tau)$ represents the prediction probability that window τ belongs to the c type of operating condition, b_c represents the class bias, r_c represents the class prototype vector, T represents the temperature coefficient, and C represents the number of state classes. The

equation controls the smoothness of the probability distribution through the temperature coefficient, so that similar states such as flow attenuation and seal leakage, pressure fluctuation and pipeline disturbance are not prematurely pressed into a single category.

The training phase needs to deal with imbalanced fault samples. The proportion of normal operation data is usually high, and the samples of seal leakage and early vibration of bearings are few. If ordinary cross entropy is used, the model is easy to bias to the normal category. In order to reduce the weakening risk of a few fault categories in training, the loss function introduces class weight and difficult sample adjustment term and enhances the classification constraint, as shown in the following equation:

$$\mathcal{L}_{\mathrm{cls}} = -\frac{1}{\mathrm{B}}\sum_{\tau=1}^{\mathrm{B}}\sum_{c=0}^{\mathrm{C}-1}\omega_{c}\, y_{\tau c}(1-\hat{p}_{c}(\tau))^{\delta}\log(\hat{p}_{c}(\tau)+\epsilon) \tag{13}$$

Here, $\mathcal{L}_{\mathrm{cls}}$ represents the classification loss, B represents the batch number of samples, ω_{c} represents the sample weight of class c, δ represents the hard sample adjustment coefficient,$y_{\tau c}$ represents the one-hot encoding of the true label of the sample, and $\hat{p}_{c}(\tau)$ represents the prediction probability. This formula makes the fault samples with low confidence obtain higher gradient contribution in training, and avoids the model only learning the high-frequency normal state.

For valve-cooled main circulation pumps, where slight flow attenuation and early bearing anomalies tend to be small in number, but engineering risks are high, this loss structure is able to retain the learning strength of such samples. The classification probabilities also need to be transformed into continuous risk values that can be used for station-end system reading. In this paper, the abnormal probability, the maximum fault probability difference, the continuous window change rate and the sensor confidence are combined into a risk score. In order to form a continuous risk value that can be used in the station alarm interface, the model synthetically combines category probability and trend change to construct a score and connect the output module, as shown in the following equation:

$$q(\tau) = \psi_{1}(1-\hat{p}_{0}(\tau)) + \psi_{2}\max_{c>0}\hat{p}_{c}(\tau) + \psi_{3}\|\Delta g_{\tau}\|_{2} - \psi_{4}\zeta_{\tau} \tag{14}$$

Here, $q(\tau)$ represents the risk score of window τ, $\hat{p}_{0}(\tau)$ represents the normal class probability, $\max_{c>0}\hat{p}_{c}(\tau)$ represents the maximum fault class probability, Δg_{τ} represents the graph-level represents the amount of adjacent window variation, ζ_{τ} represents the sensor confidence, and ψ_{1} to ψ_{4} are the scoring weights. This formula makes the alarm result not only depend on the single classification probability, but also absorb the trend change and data credibility.

When the sensor confidence decreases, the score is suppressed to avoid misjudgment caused by abnormal sampling. The final discrimination needs to output both the fault category and the alarm level. The station system not only needs to know the prediction result of the model, but also needs to identify whether the result enters the reminding, early warning or shutdown review interval. In order to ensure that the classification results can enter the operation and maintenance process, the system gives the final judgment and forms the output layer based on the risk score and class probability, as shown in the following equation:

$$\hat{y}(\tau) = \arg\max_{c} \hat{p}_c(\tau), \quad L(\tau) = \begin{cases} 0, & q(\tau) < \theta_1 \\ 1, & \theta_1 \le q(\tau) < \theta_2 \\ 2, & \theta_2 \le q(\tau) < \theta_3 \\ 3, & q(\tau) \ge \theta_3 \end{cases} \tag{15}$$

Here, $\hat{y}(\tau)$ represents the final fault category, $L(\tau)$ represents the alarm level, and θ_1 to θ_3 are the risk partition thresholds. Windows below θ_1 are classified into the normal monitoring area, Windows between θ_1 and θ_2 are classified into the reminder area, Windows between θ_2 and θ_3 are classified into the warning area, and Windows above θ_3 are classified into the shutdown review area.

This rule connects the model output with the on-site disposal process, so that the calculation results can be entered into the operation and maintenance platform of the valve cooling system of the converter station. The class probability, risk score, alarm level and trigger measurement points generated by the classification algorithm are written into the detection log synchronously, and the window index, pump number and measurement point combination are also retained, so that each alarm can be corresponding to the specific main circulation pump and its operation segment. The output records and training samples were uniformly numbered to facilitate subsequent review, fault traceability and model retraining. The detection log can also be used for operation report generation and multi-site sample migration, so that the improved graph convolutional neural network can form a complete calculation link from graph feature propagation to fault discrimination, from alarm output to result backtracking, and provide a landing algorithm support for online identification of abnormal working conditions of the main circulation pump.

4 Results

4.1 Experimental Design

The fault detection experiment of the main circulation pump of the valve cooling system in the converter station is based on the synchronous operation data at the station end. The data are from the valve cooling main circulation pump monitoring system of two converter stations, which contains 38,640 valid records. The sampling content covers measurement points such as inlet pressure, outlet pressure, mother tube flow, motor current, pump body vibration and cooling medium temperature, and calibration is completed according to maintenance records, alarm logs and operation curves. The sample categories include normal operation, flow attenuation, pressure fluctuation, bearing vibration, seal leakage, and motor current anomaly. All the records were aligned in chronological order, the abnormal shortage segment was filled by the adjacent stable window, and the obvious communication interruption segment did not enter the training set. The dataset is divided into training set, validation set and test set at 8:1:1, and the test set is kept independent and does not participate in neighboring weight learning.

As shown in Table 2, the experimental setup revolves around the multi-point plot structure input.

Table 2: Experimental data and model parameter Settings

Item	Setting	Description
Data scale	38,640 records	Covers pump units from two converter stations
Input measuring points	Pressure, flow, current, vibration, temperature	Constructs state graph nodes
State categories	6 classes	Corresponds to normal operation and five fault types
Data split	8:1:1	Used for training, validation, and testing
Comparative models	SVM, CNN-LSTM, GCN, IGCN	Verifies the effectiveness of the graph convolution structure
Evaluation metrics	Accuracy, Recall, F1-score, Delay	Measures detection performance and response efficiency

The improved graph convolutional neural network takes the windowed fault feature map as the sample, and each window contains the node feature matrix, dynamic adjacency matrix and state label. The node feature is composed of the amplitude mean, fluctuation variance, change slope and frequency band energy, and the adjacency matrix is generated by the correlation of measurement points, connection distance and response delay. The model uses Adam optimizer, initial learning rate 0.001, batch size 64, and 120 rounds of training. The validation set is used to adjust the smoothing coefficients, temperature parameters and classification thresholds, and the test set is used to evaluate the final performance. The comparison models are selected as SVM, CNN-LSTM and GCN, representing shallow classification, temporal deep learning and basic graph convolutional structures. The experimental platform is implemented with Python3.10 and PyTorch, the graph structure operation is completed in the GPU environment, and the average delay of a single window is recorded in the inference stage. The design can test the learning ability of the model for the coupling relationship between the measuring points of the valve cold pump and the stability of fault identification.

4.2 Experimental Results

The experimental results focus on the main circulation pump fault detection accuracy, category recognition stability, graph structure contribution and online response ability. The test sets were kept independent and all models read the same batch of normalized window samples. SVM takes artificial statistical features as input, CNN-LSTM reads multi-channel time series, ordinary GCN reads fixed adjacency matrix, and IGCN reads dynamic fault feature map. The outputs of the four types of models are mapped into six types of states: normal operation, flow attenuation, pressure fluctuation, bearing vibration, seal leakage and motor current anomaly. During the experiment, the dynamic adjacency matrix of the valve cold pump measurement point map is updated once per window, and the classification layer synchronously outputs the class probability, risk score and alarm level. The evaluation results not only record the final category, but also retain the trigger measurement point, window number and inference time, so that the model detection results can correspond to specific pump groups and specific operation segments.

To compare the overall detection ability of different models on the test set, Table 3 lists the accuracy, recall, F1-score, and average inference delay. The precision of IGCN is 96.1%, the recall rate is 94.8%, the F1-score is 95.6%, and the average inference delay is 38ms.

Compared with ordinary GCN, IGCN improves F1-score by 3.4 percentage points and only increases delay by 4ms, indicating that dynamic edge weights and residual propagation do not weaken online detection efficiency. SVM has fast inference speed, but artificial features are difficult to express the conduction relationship of measurement points. CNN-LSTM can capture time dependence, but regard each measurement point as a parallel channel. The performance of ordinary GCN is significantly improved after introducing topological expression, but the adaptability of fixed adjacency matrix to operating condition switching is insufficient.

Table 3: Comparison of the overall detection performance of different models

Model	Accuracy/%	Recall/%	F1-score/%	Delay/ms
SVM	87.4	84.9	85.7	18
CNN-LSTM	91.6	89.7	90.4	42
GCN	93.2	91.5	92.2	34
IGCN	96.1	94.8	95.6	38

The stage distribution of training loss, validation loss and validation accuracy can reflect the learning stability of IGCN, as shown in Fig. 6. The training loss is reduced from 0.482 to 0.037, the validation loss is reduced from 0.506 to 0.061, and the validation accuracy is stable above 95.8% after the 86th round. The first 40 rounds of the box body is wide, indicating that the pressure, flow and current measurement point correlation is still in the learning stage. The median loss of the 41st to the 80th round continued to decrease, and the box gradually contracted. The accuracy of 81-120 rounds is concentrated in the high value interval, which indicates that the dynamic adjacency update and timing residual aggregation do not introduce obvious oscillation, and can weaken the influence of short-term disturbance of the pump group on the classification results.

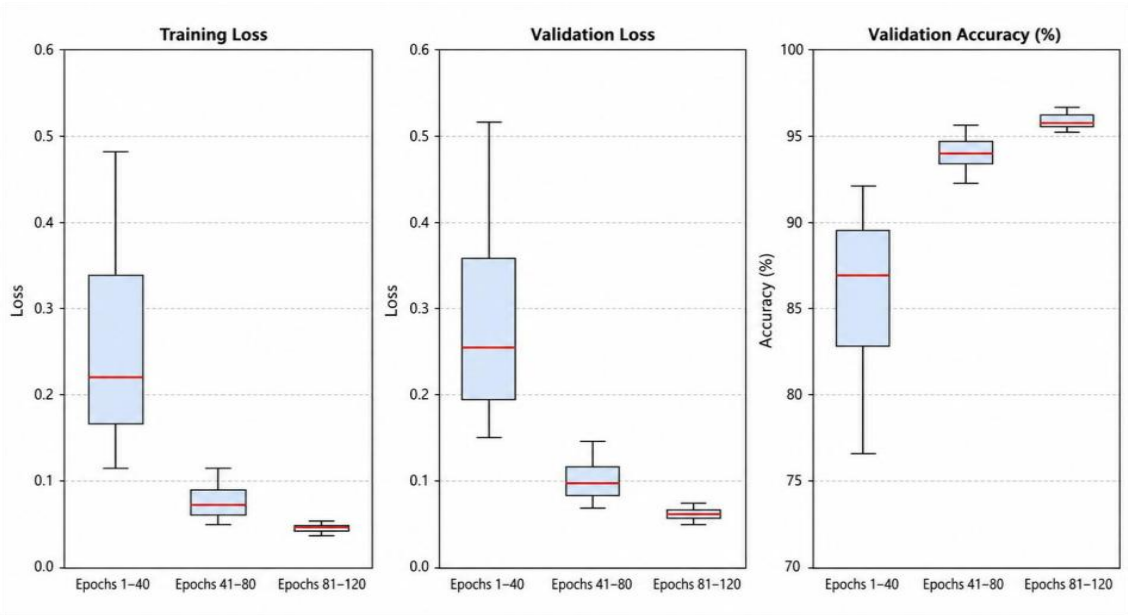

Figure 6: Box distribution plot of loss versus validation accuracy during IGCN training

Table 4 lists the detection results for each fault category. The recall rate of seal leakage is 93.2%, which is lower than bearing vibration and motor current anomalies, but still higher than the 90.5% of CNN-LSTM in similar samples. The F1-score of the pressure fluctuation

category reaches 94.7%, indicating that graph convolution has a strong ability to express the linkage characteristics between inlet pressure, outlet pressure and mother tube flow. The results show that IGCN does not rely on a single measurement point anomaly to make a judgment, but uses the graph-level representation after measurement point topology propagation to complete the classification. The accuracy of bearing vibration and motor current anomalies reaches 96.2% and 96.8%, respectively, indicating that the correlation propagation between electromechanical link nodes can enhance the ability of the model to discriminate rotating component anomalies. The indicators of flow attenuation and seal leakage are slightly lower, reflecting that the two types of states have similar hydraulic responses in the early stages.

Table 4: Classification knots of IGCN in different main circulation pump states

State Category	Precision/%	Recall/%	F1-score/%
Normal operation	97.9	98.1	98.0
Flow attenuation	94.1	93.7	93.9
Pressure fluctuation	95.0	94.5	94.7
Bearing vibration	96.2	95.7	95.9
Seal leakage	93.8	93.2	93.5
Motor current abnormality	96.8	96.4	96.6

The confusion matrix further illustrates the ability of the model to distinguish different fault classes. In Fig. 7, a heat map is used to show the identification distribution of the six types of states, and the main diagonal proportions of normal operation, bearing vibration and motor current anomaly are 98.1%, 95.7% and 96.4%, respectively. There is still a small amount of cross between flow attenuation and seal leakage, mainly from the two types of faults will cause the flow decline of the mother tube and the slow change of the outlet pressure. Since IGCN reads the propagation results of pressure, flow and current nodes simultaneously, this crossover ratio is controlled within 3.1%. The pressure fluctuation samples in the heat map are mainly concentrated in the diagonal region, which indicates that the edge weight update of the inlet pressure and outlet pressure nodes can effectively distinguish the pipeline disturbance and the pump body degradation.

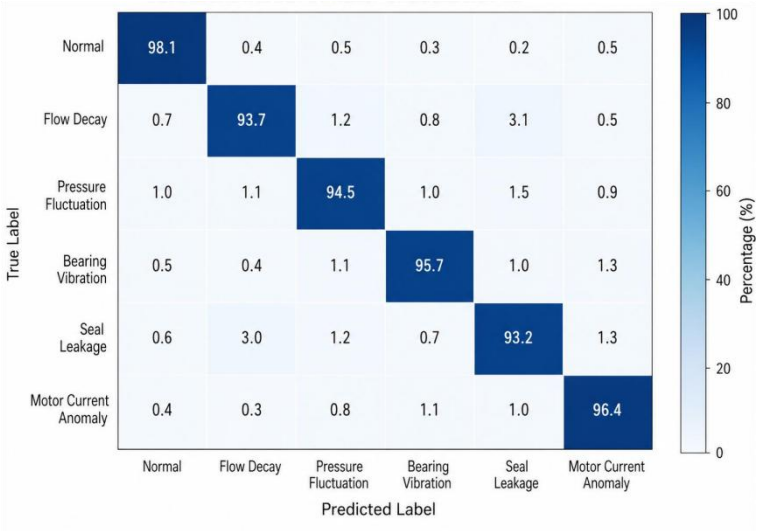

Figure 7: Heatmap of confusion matrix for identification of six classes of states of the main circulation pump

Ablation experiments are used to verify the contribution of each module to the results, as shown in Table 5, removing dynamic adjacency update, time series residual aggregation, measurement point topology mapping, and association attention propagation, respectively. After removing the dynamic adjacency update, the Accuracy drops to 93.8%, which indicates that the fixed topology is difficult to adapt to the cooling load change. After removing the timing residual aggregation, the Recall decreased to 92.9%, and the missed detection of bearing vibration and pressure fluctuation samples increased. After removing the topological mapping of measurement points, the model degenerates to ordinary multi-channel input, and the F1-score decreases to 91.6%, which proves that the graph structure is the main source of performance of the proposed method. After removing the association attention propagation, the model can still complete the classification, but the confusion between the flow attenuation and sealed leakage samples increases, which indicates that the node contribution allocation has the distinguishing value for similar faults.

Table 5: Results of IGCN ablation experiments

Model Setting	Accuracy/%	Recall/%	F1-score/%	Delay/ms
Without dynamic adjacency update	93.8	92.1	92.7	35
Without temporal residual aggregation	94.2	92.9	93.4	36
Without measuring-point topology mapping	92.4	90.8	91.6	31
Without relational attention propagation	94.6	93.1	93.9	37
Complete IGCN	96.1	94.8	95.6	38

Fig. 8 shows the ROC curves of different models in multi-class fault detection. The macro-average AUC of IGCN is 0.982, which is higher than 0.956 of GCN and 0.931 of CNN-LSTM. The curve maintains a high true positive rate in the low false positive rate interval, which indicates that the model has a good margin of discrimination in the early alarm scenario. This result is consistent with the recall change in Table 3, which also indicates that the dynamic adjacency matrix is able to enhance the separability of the slight fault samples. When the false positive rate is lower than 0.08, the IGCN curve still maintains a significant upward trend, which is suitable for the operation scenario where the station alarm system has high requirements for missed detection control.

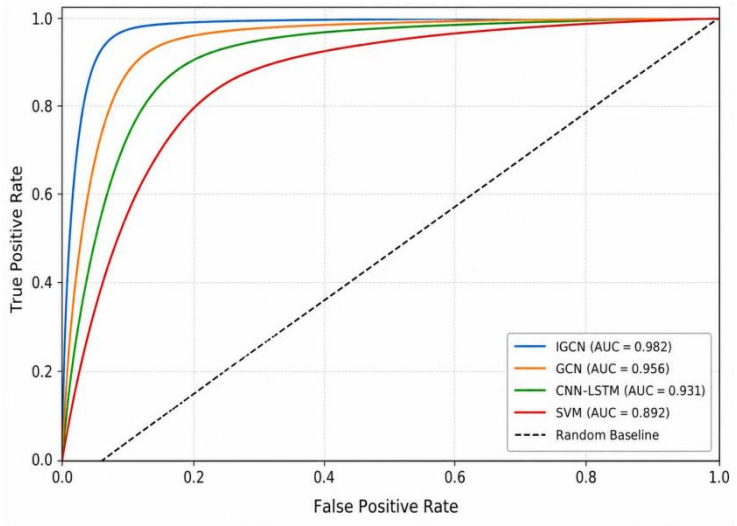

Figure 8: Multi-class fault detection ROC curves for different models

From the perspective of inference efficiency, the 38ms delay of the complete IGCN is lower than the sampling period of seconds at the station end, which can meet the calculation rhythm of continuous monitoring of the main circulation pump. Although its delay is higher than that of SVM and ordinary GCN, the additional time mainly comes from the update of adjacency matrix and the calculation of node attention weight, and the performance gain in exchange is more suitable for the requirements of valve-cooled system for early fault identification. The model does not rely on manual rule correction in the testing phase, and all results are directly generated by the graph feature propagation and classification layer, which shows that the method has end-to-end detection ability.

Comprehensive experimental results show that IGCN can complete multi-class fault recognition of main circulation pump while maintaining millisecond reasoning speed. The performance advantage comes from the collaborative computation of the measurement point topology, dynamic edge weights, and timing residuals. For the valve cooling system of converter station, the model can convert scattered pressure, flow, current, vibration and temperature data into learnable graph structure results, and output traceable fault categories and alarm basis. Compared with the monitoring method relying on a fixed threshold, IGCN is more suitable for describing the pump group state under the common change of multiple measurement points. Compared with ordinary deep networks, the graph structure preserves the engineering connections in the valve cooling loop. In the actual operation and maintenance records, the pressure fluctuation and flow attenuation often appear before the manual alarm. The model can retain this sequence in the window level results, which is convenient for operators to check the status of pump body, valve and pipeline according to the trigger measurement point. At the same time, the class probability and risk score in the log can support the subsequent model re-training, so that the new samples continue to enter the detection closed loop. The overall results have engineering interpretability, and provide a stable and reliable measured data basis for the intelligent monitoring of the valve cold pump in the converter station.

4.3 Discussion

Compared with SVM, CNN-LSTM and ordinary GCN, IGCN reflects a stronger expression ability of measurement point correlation in the fault detection of valve-cooled main circulation pump. Experimental results show that the Accuracy of IGCN reaches 96.1%, the Recall reaches 94.8%, the F1-score reaches 95.6%, and the average inference delay is 38ms, which are higher than 93.2%, 91.5% and 92.2% of GCN, and also significantly better than CNN-LSTM and SVM. In the confusion matrix, the recognition proportions of normal operation, bearing vibration and motor current abnormality were 98.1%, 95.7%and 96.4%respectively, indicating that the measurement points of the electromechanical link formed a clear category boundary after graph convolution propagation. There is still a small cross between the flow attenuation and the seal leakage, mainly because both types of states will cause the flow decline of the mother tube and the slow change of the outlet pressure. Ablation experiments show that the F1-score is reduced to 91.6% after removing the topological mapping of measurement points, and the Accuracy is reduced to 93.8% after removing the dynamic adjacency update, indicating that the graph structure and edge weight update are the source of model performance. Compared with the fixed threshold and the ordinary time series model, IGCN converts the pressure, flow, current, vibration and temperature into learnable nodes, and retains the operation coupling relationship in the dynamic adjacency matrix, so that the alarm results can be traced back to the trigger measurement point and the specific window, which has good engineering review value. The results show that the on-line diagnosis of valve-cold pump needs to consider the change of

operation data, the spatial position of measurement points and the direction of fault propagation. After integrating the relationship of multiple measurement points into the same graph structure, the classification process can retain the correlation path formed by the fault, and the output results are more suitable for station review and continuous monitoring.

5 Conclusion

In this paper, an improved graph convolutional neural network model is constructed around the fault detection task of the main circulation pump of the valve cooling system of the converter station. In the model, pressure, flow, motor current, vibration and temperature measurement points are transformed into graph nodes, operation correlation, equipment connection relationship and abnormal response are sequentially written into the adjacency structure, and short-term fluctuations are retained by time series residual aggregation. Compared with the methods relying on a fixed threshold or a single channel sequence, the proposed model can express the relationship among hydraulic links, electromechanical links and thermal response links in the calculation process, so that the fault identification does not stop at a single point over-limit judgment. The limitations of this paper are mainly reflected in the limited range of sample sources, the boundary overlap between some early fault states and similar working conditions, and the additional computational load caused by dynamic adjacency update. The follow-up research can be carried out from three directions. Firstly, more operation samples of converter stations and different pump types are introduced to enhance the adaptation ability of the model in cross-site scenarios. The concept drift detection and online update mechanism were combined to make the model adapt to seasonal load, cooling medium temperature and pump group working conditions. The lightweight graph convolution structure was designed to reduce the inference pressure at the edge end. In the future, the alarm log interpretation mechanism can be further improved, and the trigger detection point, propagation path and maintenance conclusion can be correlated, so that the model output is more suitable for on-site review and continuous training. At the engineering application level, the model also needs to be further connected with the station monitoring system, historical maintenance records and operation and maintenance processes to form a closed-loop link from signal reading, graph structure generation, fault discrimination to disposal records. This link can reduce the pressure of manual review, and enhance the traceability of detection results and application reliability.

Funding

This work was supported by the Technical improvement project of China Southern Power Grid Co., Ltd. under Grants 011000SB24030002.

References

[1] Cheng W, Wang S, Zhang L, et al. Unsupervised planetary gearbox fault detection for nuclear circulating water pump based on generalized features[J]. IEEE Transactions on Instrumentation and Measurement, 2024, 73: 1-10.

[2] Zhang X, Jiang L, Wang L, et al. A pruned-optimized weighted graph convolutional network for axial flow pump fault diagnosis with hydrophone signals[J]. Advanced Engineering Informatics, 2024, 60: 102365.

[3] Kovalenko A, Pozdnyakov V, Makarov I. Graph neural networks with trainable adjacency matrices for fault diagnosis on multivariate sensor data[J]. IEEE Access, 2024, 12: 152860-152872.

[4] Brahmbhatt P, Patel R, Maheshwari A, et al. Improved fault detection and diagnosis using graph auto encoder and attention-based graph convolution networks[J]. Digital Chemical Engineering, 2024, 11: 100158.

[5] Seo J, Noh Y, Kang Y J, et al. Graph neural networks for anomaly detection and diagnosis in hydrogen extraction systems[J]. Engineering Applications of Artificial Intelligence, 2024, 135: 108846.

[6] Zaman W, Ahmad Z, Kim J M. Fault diagnosis in centrifugal pumps: A dual-scalogram approach with convolution autoencoder and artificial neural network[J]. Sensors, 2024, 24(3): 851.

[7] Ullah N, Ahmad Z, Siddique M F, et al. An intelligent framework for fault diagnosis of centrifugal pump leveraging wavelet coherence analysis and deep learning[J]. Sensors, 2023, 23(21): 8850.

[8] Manikandan S, Duraivelu K. Vibration-based fault diagnosis of broken impeller and mechanical seal failure in industrial mono-block centrifugal pumps using deep convolutional neural network[J]. Journal of Vibration Engineering & Technologies, 2023, 11(1): 141-152.

[9] Ahmad Z, Kim J Y, Kim J M. A technique for centrifugal pump fault detection and identification based on a novel fault-specific Mann–Whitney test[J]. Sensors, 2023, 23(22): 9090.

[10] Zaman W, Ahmad Z, Siddique M F, et al. Centrifugal pump fault diagnosis based on a novel SobelEdge scalogram and CNN[J]. Sensors, 2023, 23(11): 5255.

[11] Ahmad S, Ahmad Z, Kim J M. A centrifugal pump fault diagnosis framework based on supervised contrastive learning[J]. Sensors, 2022, 22(17): 6448.

[12] Maliuk A S, Ahmad Z, Kim J M. Hybrid feature selection framework for bearing fault diagnosis based on wrapper-WPT[J]. Machines, 2022, 10(12): 1204.

[13] Afridi Y S, Hasan L, Ullah R, et al. LSTM-based condition monitoring and fault prognostics of rolling element bearings using raw vibrational data[J]. Machines, 2023, 11(5): 531.

[14] Zabin M, Choi H J, Uddin J. Hybrid deep transfer learning architecture for industrial fault diagnosis using Hilbert transform and DCNN–LSTM: M. Zabin et al[J]. The Journal of supercomputing, 2023, 79(5): 5181-5200.

[15] Siddique M F, Zaman W, Ullah S, et al. Advanced bearing-fault diagnosis and classification using mel-scalograms and FOX-optimized ANN[J]. Sensors, 2024, 24(22): 7303.

[16] Zaman W, Siddique M F, Ullah S, et al. Hybrid deep learning model for fault diagnosis

in centrifugal pumps: A comparative study of VGG16, ResNet50, and wavelet coherence analysis[J]. Machines, 2024, 12(12): 905.

[17] Umar M, Siddique M F, Ullah N, et al. Milling machine fault diagnosis using acoustic emission and hybrid deep learning with feature optimization[J]. Applied Sciences, 2024, 14(22): 10404.

[18] Praveen Kumar T, Buvaanesh R, Saimurugan M, et al. Performance evaluation of deep learning approaches for fault diagnosis of rotational mechanical systems using vibration, sound, and acoustic emission signals[J]. Journal of Low Frequency Noise, Vibration and Active Control, 2024, 43(3): 1363-1380.

[19] Al-Andoli M N, Tan S C, Sim K S, et al. A parallel ensemble learning model for fault detection and diagnosis of industrial machinery[J]. IEEE Access, 2023, 11: 39866-39878.

[20] Bonci A, Fredianelli L, Kermenov R, et al. Deepesn neural networks for industrial predictive maintenance through anomaly detection from production energy data[J]. Applied Sciences, 2024, 14(19): 8686.

[21] Kermenov R, Nabissi G, Longhi S, et al. Anomaly detection and concept drift adaptation for dynamic systems: a general method with practical implementation using an industrial collaborative robot[J]. Sensors, 2023, 23(6): 3260.